GEOPHYSICS, VOL. 73, NO. 4 (JULY-AUGUST 2008); P. E145–E152, 13 FIGS., 1 TABLE.
10.1190/1.2940154

Case History

Acoustic signatures of crossflow behind casing in commingled reservoirs: A case study from Teapot Dome

Andrey Bakulin[1] and Valeri Korneev[2]

ABSTRACT

Cracks and channels in cement often create unwanted conduits behind casing that lead to crossflow between different producing zones. Crossflow results in lost production or aquifer contamination because fluid flows from a higher-pressure to a lower-pressure zone instead of traveling up the well. We present measurements of acoustic signatures of crossflow behind the pipe in time and frequency domains. Despite being called "noise," they are shown to be propagating tube waves with impulsive signatures. When multiple crossflow locations are present along the well, these signatures are unique for each location and are highly repeatable. We observe time-lapse change in such signatures during air injection and release and suggest that these changes can be used for real-time acoustic characterization of depletion in stacked commingled reservoirs. We anticipate that such signals are typical for commingled production of multilayered reservoirs. Acoustic signatures can be used to characterize crossflow and depletion. In addition, crossflow signals represent a strong noise affecting downhole seismic surveillance with active sources.

INTRODUCTION

Permanent acoustic and seismic monitoring in production and injection wells is an emerging area of reservoir surveillance. To make it successful, one needs good knowledge about sources of abundant natural sound in flowing or shut-in wells that penetrate multilayered producing reservoirs. These natural noises can be considered useful signals for characterizing various flow conditions or production problems. For downhole surveillance with active sources, these noises represent an obstacle that needs to be overcome, for instance, by stacking. In any case, a good road map of the downhole "acoustic kingdom" is essential for active or passive acoustic/seismic surveillance. This study reports such an experimental investigation that reveals strong abundant impulsive signals that turned out to be time-domain expressions of crossflow "noises" typical of commingled reservoirs.

Crossflow behind the pipe generates a distinct acoustic response, formerly named *noise*. Noise logging used single-sensor passive listening and was used to detect flow through poor-quality cement behind casing (McKinley et al., 1973). The signature measured downhole was peak-to-peak or averaged amplitude over a long observation time of about 60 s. The higher the noise level, the closer the sensor was to the leak location. In addition, the spectral distribution of acoustic energy was used for discrimination of one- and two-phase flow. Because this acoustic signature was considered noise, no attempt was made to record seismograms in the time domain. Such an approach mixes all signals from various crossflow locations. Mixing and averaging can be useful to characterize flow regimes (van der Spek and Thomas, 1999) using statistical methods. Our experiments suggest that crossflow signatures have a strong deterministic component that could be revealed easily with multisensor arrays and used to extract additional information about location and types of crossflow sources. We also foresee that strong crossflow signals can be a challenge for downhole surveillance with active man-made sources.

FIELD EXPERIMENT

Passive downhole listening has been performed in a dedicated small-diameter well (microhole) at Teapot Dome oil field, Natrona County, Wyoming. This field represents Naval Petroleum Reserve #3, operated by the Rocky Mountain Oilfield Testing Center of the U. S. Department of Energy. The microhole was drilled by Los Ala-

Manuscript received by the Editor 30 August 2007; revised manuscript received 15 January 2008; published online 16 July 2008.
[1]Formerly Shell International Exploration and Production Inc.; presently WesternGeco, Houston, Texas, U.S.A. E-mail: abakulin@slb.com.
[2]Lawrence Berkeley National Laboratory, Berkeley, California, U.S.A. E-mail: vakorneev@lbl.gov.

mos National Laboratory within the framework of the U. S. Department of Energy microhole initiative (U. S. Department of Energy, 2007) and is located 15 m from producing well NPR #3 67 SX 34 (Figure 1). Production occurs from two Upper Cretaceous reservoirs represented by upper and lower Shannon bioturbated shelf sandstones (Tomutsa et al., 1986). The upper Shannon has higher porosity and permeability (Tomutsa et al., 1986) and is separated from the lower Shannon by a low-permeability bioturbated shelf siltstone. Figure 2 shows various log measurements taken in this well.

The producing well has perforations in both upper and lower Shannon, and production is commingled. Figure 3 shows the sketch and wellhead of the microhole. It has three casing strings all cemented to the surface: internal plastic string to 244 m, steel casing to 179 m, and steel conductor to 12 m. A 20-level hydrophone array with spacing of 5 m was used for recording. The array was placed at three depth settings to cover the entire well. Microhole casing had no perforations and was filled to the top with water.

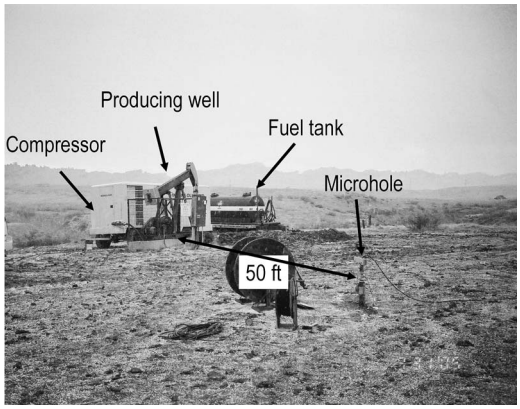

Figure 1. Field-experiment layout with producing well and microhole.

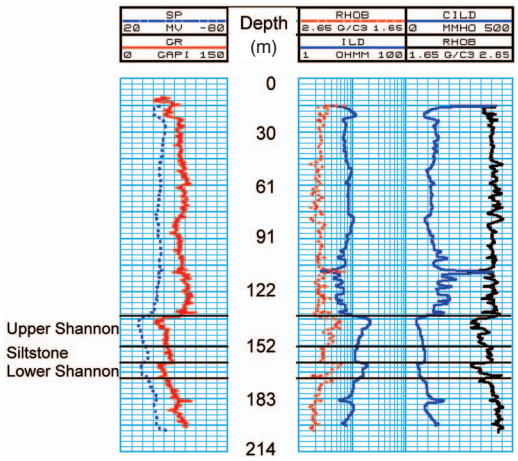

Figure 2. Well logs from NPR #3 67 SX 34 showing location of upper and lower Shannon sandstone reservoirs separated by a low-permeability siltstone. GR — gamma ray; SP — spontaneous potential log; RHOB — bulk-density log; ILD — induction-resistivity log; CILD — deep-reading induction-resistivity log. Black lines show interpreted depths of the upper and lower Shannon.

NOISE SIGNATURES

Seismic recording in the absence of any active source has revealed very coherent events, shown in Figure 4. For a short recording time (2 s), these events were not always present and had an irregular occurrence on repeated recordings. Low frequencies (<1000 Hz), linear moveout, and velocity of ~950–1000 m/s suggest that these are tube waves, which was verified by later experiments with the active source. Numerical modeling also confirms these conclusions. As shown by Paillet and White (1982), a tube wave is the only symmetric mode that exists between zero and the cutoff frequency for a next mode. In a simplified model of a microhole (Table 1), the cutoff frequency for the next symmetric mode is estimated at ~1680 Hz. At low frequencies, the dispersion curve for the tube wave is shown in Figure 5. Low tube-wave velocity is a result of the small microhole diameter and slow-velocity material of PVC casing. Although predicted velocity is ~900 m/s, in experiments, we observe faster speeds of 950–1000 m/s because of the presence of additional casing string. Although the tube wave does not attenuate in fast formations or steel-cased boreholes, we observe substantial attenuation in the microhole because shear velocity of PVC as well as formation is lower than acoustic velocity in the water.

Triangle-shaped arrivals consist of upgoing and downgoing tube waves with an apex that represents an apparent source location (Figure 4). The majority of similar triangular events originated in or around both reservoirs. These events have a clear impulsive nature, as if air guns had excited them. Long records reveal that the event

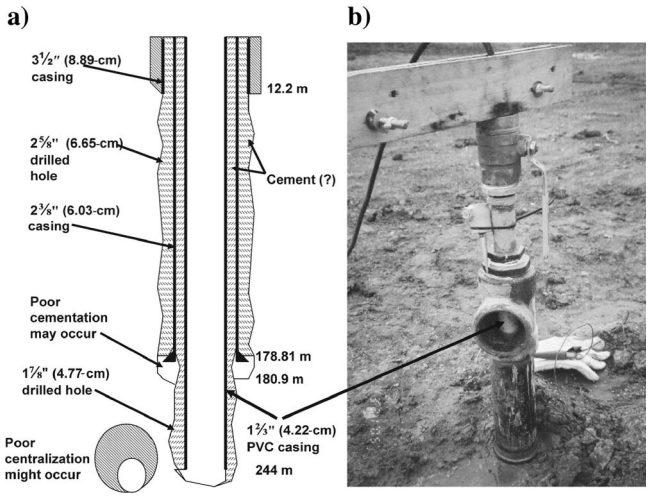

Figure 3. (a) Sketch of the microhole and (b) photo of its wellhead.

Table 1. Geometry and elastic properties for simplified three-layer microhole model. Note that the model assumes lossless materials.

Cylindrical layers	Material	Outer radius (mm)	Longitudinal velocity (m/s)	Shear velocity (m/s)	Density, (kg/m^3)
Layer 1	Water	37	1500	0	1000
Layer 2	PVC	42	1800	600	1400
Layer 3	Formation	Infinite	2600	800	2400

waveforms from the same depths are very repeatable (Figure 6).

Four hypotheses were considered to explain the origin of the repeated events:

1) mechanical noise from the surface
2) signals from neighboring pump jacks propagating horizontally along the reservoir
3) horizontally propagating waves from gas bubbles bursting in the vicinity of the closest producing well
4) crossflow behind the pipe

The first three hypotheses were tested thoroughly, and none has been confirmed. Almost all beam pumps were switched off one by one in a 1000-m radius; other distant mechanical facilities on the surface were shut down. Repeated borehole measurements with and without mechanical noise sources have showed that signals of interest remain abundant and overwhelming. The third hypothesis was tested at a later stage when a neighboring producing well was subjected to three weeks of air injection. Increased reservoir pressure excluded the possibility of bubbles bursting, but the observed signals clearly remained.

The final hypothesis considers a fluid flow behind the pipe caused by a poor cementation (McKinley et al., 1973). As shown on Figure 3, there is a possibility of poor cementation in the transition section between a $2\frac{5}{8}$-in hole and a $1\frac{7}{8}$-in hole because it is a place where poor hydraulic isolation could occur (M. Cowan, personal communication, 2006). Cementation often can be problematic in conventional wells, so we can expect a larger chance of failure for inexpensive microhole drilling that is still in the experimental stage. The production logging technique called noise logging listens to passive acoustic response along the borehole and identifies location and characteristics of such leaks behind casing (McKinley et al., 1973). However, those wireline measurements are performed using a single channel and analyze amplitude spectrum which is averaged only over a long (~60-s) recording time.

Presenting our data in a similar format (Figure 7) reveals structure resembling a typical noise logging response (McKinley et al., 1973). The peak of the amplitude corresponds to the location of the flow, whereas larger energy is concentrated at lower frequencies. As an additional check, one seismic trace was converted to an audio file and played (see Appendix A). Nonexperts and petrophysical specialists (A. van der Spek, personal communication, 2006) associated

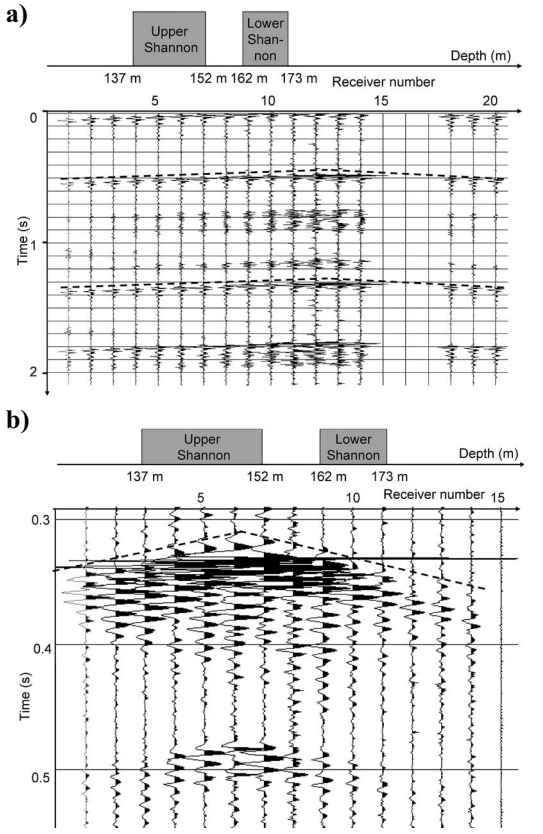

Figure 4. Triangle-shaped arrivals, recorded in a microhole, represented by upgoing and downgoing tube waves. (a) One type of event originates slightly below the lower Shannon; (b) another type of event comes from the upper Shannon. Channels 15–17 failed during the experiment.

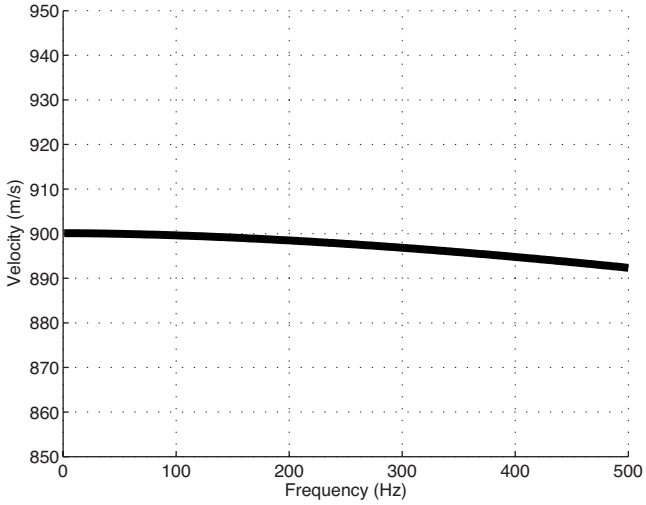

Figure 5. Dispersion curves for tube wave using simplified three-layer model of the microhole given in Table 1. Note small changes in phase velocity in a frequency band of interest.

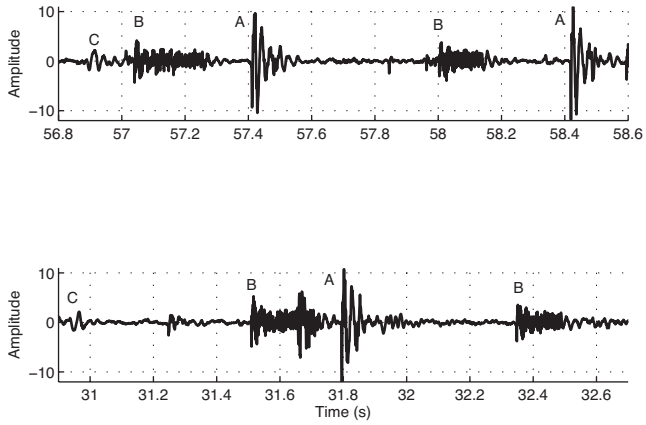

Figure 6. Parts of a longer record illustrating the repeatable character of events recorded at the same depth. The same trace from Figure A-1 is used. Events labeled as A, B, and C have different depths of origin and can be distinguished easily because of their characteristic repeatable waveforms.

these sounds with the flow through a series of constricted channels or whistling.

To simulate the artificial leak, we also measured a response excited by squeezing water out of a plastic bottle at the wellhead as well as pumping air through the plastic tubing terminating at depth (Figure 8). In all cases, we generate downgoing signals that are similar in waveform and strength to upgoing crossflow pulses (Figure 9), even though a very light squeeze on the bottle is applied. Note that in the source vicinity, natural and artificial signals are rich in high frequencies. At a distance, high frequencies are attenuated strongly, and farther from the source, only lower frequencies survive. This attenuation is likely because of the slow PVC casing that has shear velocity lower than fluid velocity, and because of the high intrinsic attenuation of PVC material. This test also confirms that recorded crossflow signals (Figure 4) indeed are represented by tube waves that have the same velocity, 950–1000 m/s.

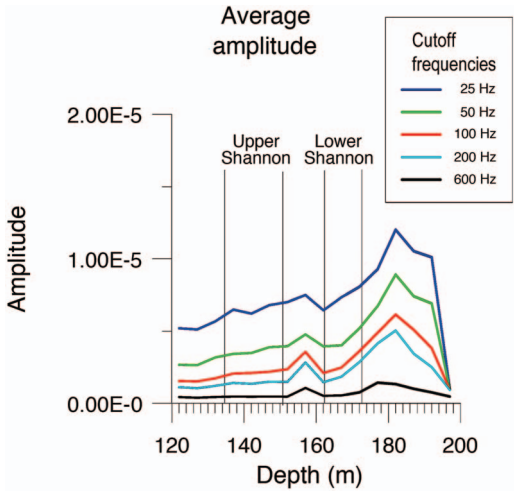

Figure 7. Average amplitude spectrum of acoustic response of crossflow as a function of depth. As offered by McKinley et al. (1973), a large spread between curves near the leak suggests two-phase or gas-to-liquid flow.

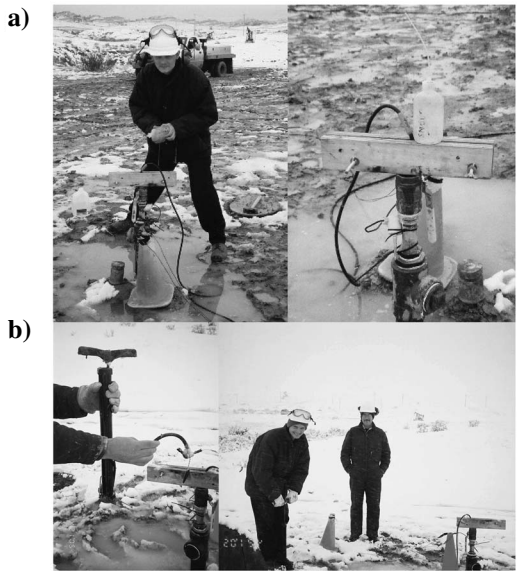

Figure 8. Simulating leaks: (a) surface leak: squeezing water-filled plastic bottle with a straw submerged into fluid at the wellhead; (b) subsurface leak: pumping air through plastic 0.13-in (0.32-cm) tubing strapped to a hydrophone array with a nozzle at 15-m depth.

TIME-LAPSE CHANGES

Observations of crossflow signatures were continued after three weeks of air injection in the former oil-producing well. After pressurizing the reservoir to as high as 300 psi (2.1 MPa), we started to release air during part of the day while keeping the well shut in at night. It was observed repeatedly that after extensive shut-in periods, the average amplitude response was always similar to that shown in

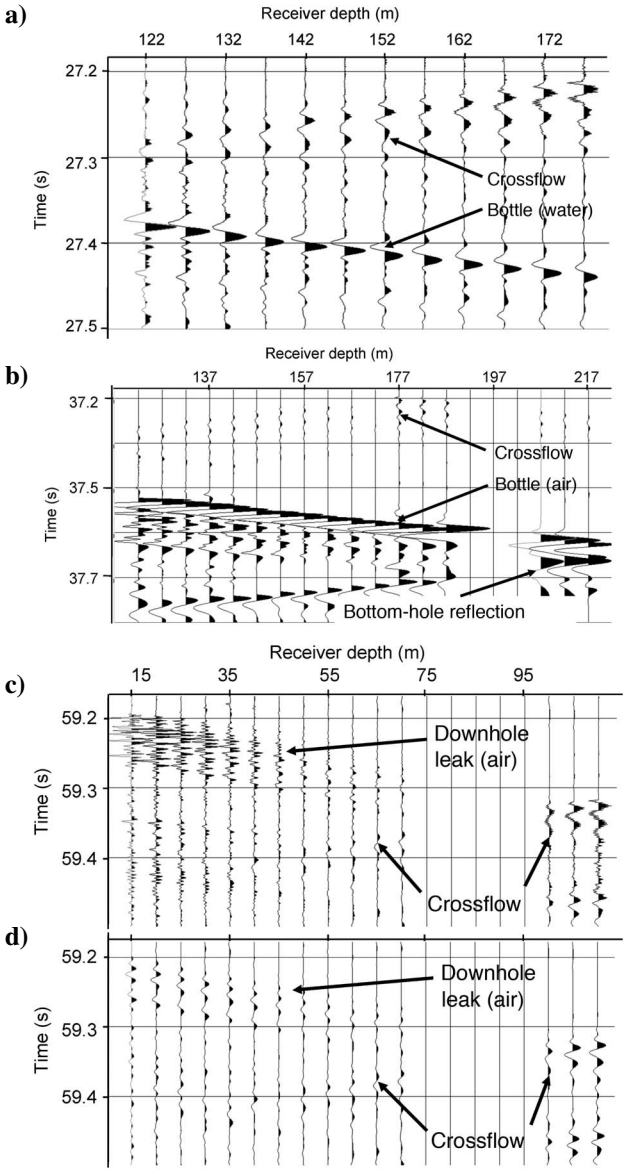

Figure 9. Comparison of natural crossflow signals with simulated leaks: bottle at the wellhead injecting (a) water and (b) air; air pumped through the plastic tubing with the nozzle at 15-m depth; (c) unfiltered and (d) band-pass-filtered 2–80 Hz. Note the similarity in propagation velocity and frequency content between natural and artificial signals.

Figure 10a, with the most energetic feature directly below the lower Shannon. When air was released for several hours, the response changed to that shown in Figure 10b, when the most energetic feature moved to directly below the upper Shannon. The next day, after an extended shut-in period, this pattern repeated (Figure 10c-f). We interpreted this pattern as a change of crossflow direction between the upper and lower Shannon.

To verify this interpretation, a simple radially symmetric reservoir model was built and history-matched with existing pressure measurements. Bottom-hole pressures were estimated by measuring a fluid level using an Echometer based on pulse-echo technique (McCoy, 1962). For reservoir modeling, the upper Shannon was described by thickness of 15 m, permeability of 40 mD, and porosity of 17%. The lower Shannon has a thickness of 11 m, permeability of

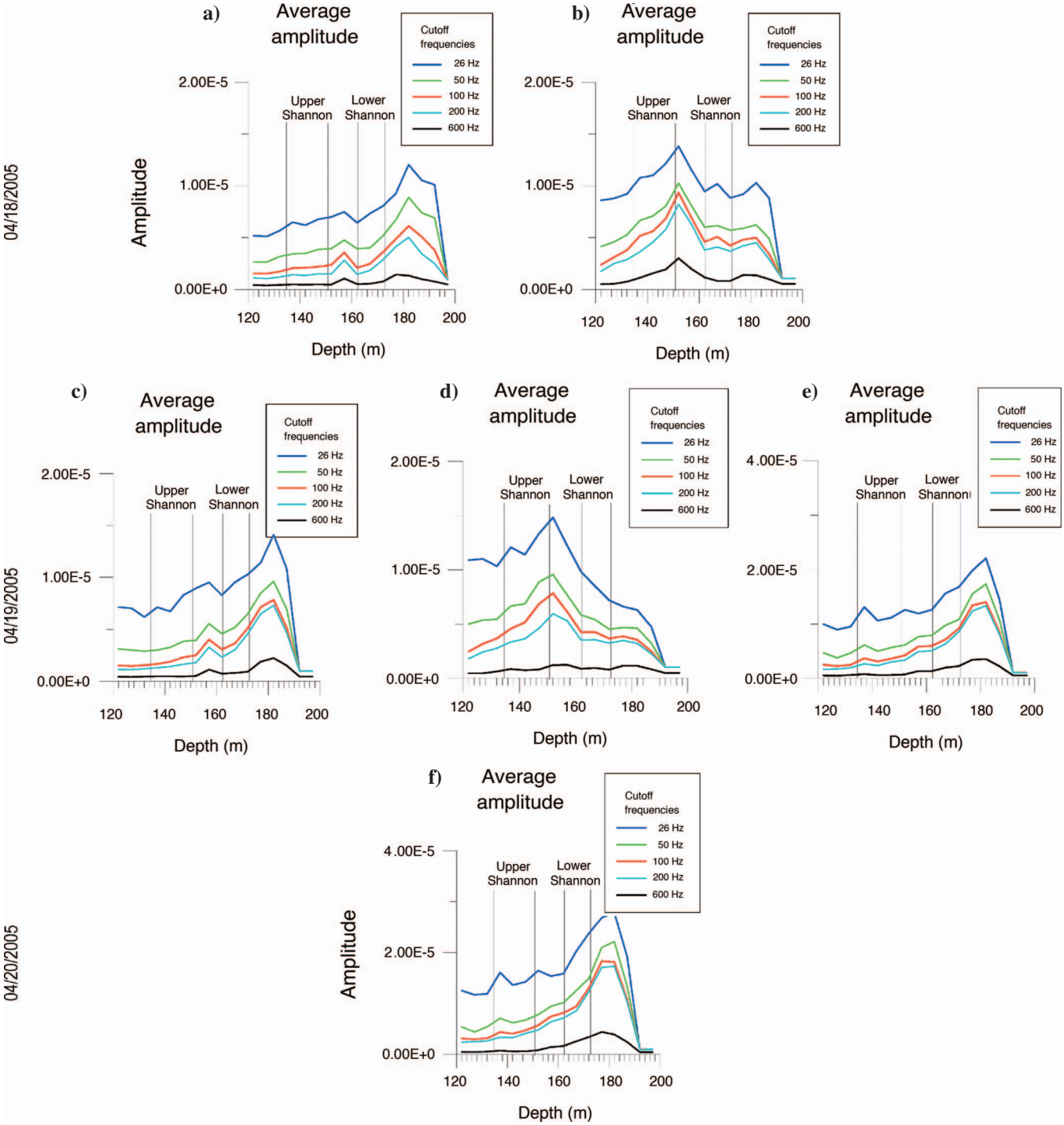

Figure 10. Changes in acoustic response of crossflow during a three-day period of cyclic air release: (a) beginning and (b) end of first day; (c) beginning, (d) middle, and (e) end of second day; (f) morning of third day. After the end of the air release, the (f) noise pattern returns back to the (a) original.

10 of mD, and porosity of 17%. Two reservoirs are separated by a 9-m layer of low permeability (0.1 mD). Porosity and permeability were taken from laboratory measurements published by Tomutsa et al. (1986).

This simple model predicts that somewhere during the air-release experiment, we should observe a change in the direction of the crossflow or a crossover between pressure curves for two reservoirs (Figure 11). The origin of this crossover can be understood from the following simple reasoning: Even for identical initial reservoir pressures, the model predicted that pressures in the upper Shannon become higher during injection. However, during air release, pressure in the upper Shannon drops faster, and during observation, it becomes lower than in the lower Shannon (Figure 11).

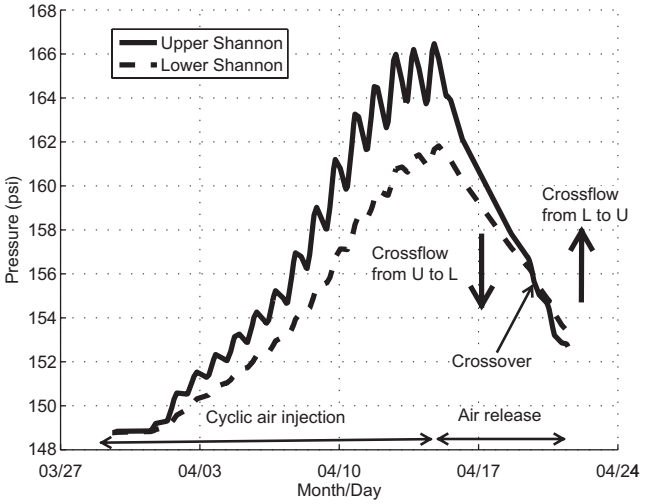

Figure 11. Pressure predicted by radially symmetric reservoir model at the location of the observation microhole. The more permeable upper Shannon builds and loses pressure at a faster rate than the lower Shannon, thus creating a crossover at the experiment observation time. Before crossover, fluid flows from the upper to lower Shannon, whereas after crossover, the flow is reversed.

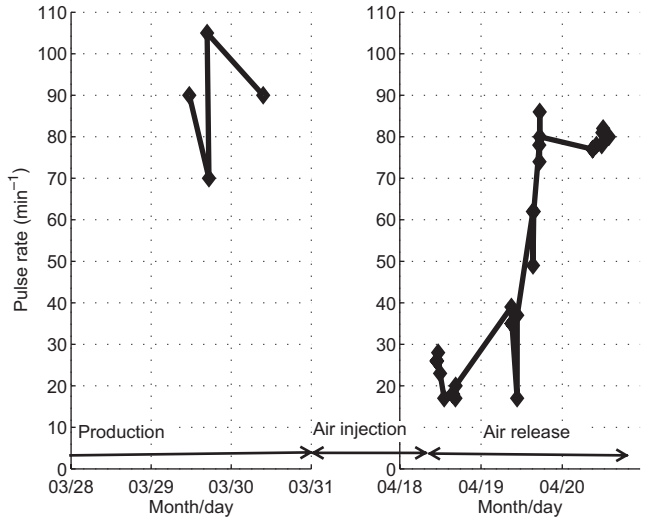

Figure 12. The rate of large-amplitude acoustic pulses is high before air injection and after air release. During air release, actual measurements are taken during brief shut-ins.

Such pressure behavior is common for commingled stacked reservoirs that have different permeability and porosity (Raghavan, 1993; Chaudhry, 2003): Pressure builds up faster in the upper Shannon reservoir with higher permeability because it can take fluid more readily. However, for the same reason, during production (air release), pressure in the upper Shannon decreases much faster. It should be stressed that the reservoir model included only the steel-cased producing wellbore that is a main conduit for crossflow between two reservoirs, whereas the microhole transmits a negligible amount of fluid behind the plastic casing and acts as a small, sensitive flow gauge that does not affect volumetric flow. Therefore, crossflow can and will occur through the main borehole itself when commingled producing zones have different reservoir properties. An intentional sidetrack or channel that penetrates several reservoir zones away from the main hole can provide a sensitive way to monitor crossflow that occurs via production holes.

As expected, a simple radial model does not predict multiple crossovers between two pressure curves. Nevertheless, it confirms that characteristic 4D changes in crossflow signatures can be explained by a change in the sign of the pressure gradient caused by crossflow that occurs between two reservoirs via the large perforated borehole.

The rate of high-amplitude pulses (Figure 12) also changed during air injection and release. Although the average pulse rate was about 90 pulse/min before air injection (end of March 2005), it became about 26 pulse/min after injection was ended (April 17, 2005). During air release, the pulse rate showed a steady increase, reaching 80 pulse/min on the third day (Figure 12), similar to what it was before injection. Because of high background noise caused by air release, measurements were taken during brief shut-ins when air release was terminated.

DISCUSSION

Modern production wells are becoming instrumented with various types of permanent sensors. The concept of "smart," or "intelligent," wells is driven by the necessity to obtain appropriate hard data in real time that can characterize well and flowing conditions and thus lead to optimization of well performance. Permanent placement of acoustic sensors is the obvious next step in this area. Passive listening can allow detection of microseismic events. Recording with an active source can be used for downhole seismic surveillance using vertical seismic profiling or crosswell seismic. To be useful, these applications require good signal-to-noise ratio. If sensors are installed in a flowing well, then flow noise inside tubing is always present.

Although this flow noise can be used to characterize the flow regime (van der Spek and Thomas, 1999), it is a major complication for microseismic and seismic surveillance. To minimize its influence, the service industry is trying to decouple permanent acoustic sensors from tubing and clamp them to the casing (Knudsen et al., 2006). This approach assumes that no major sources of noise are present behind the casing. However, crossflow creates an additional strong noise source behind the casing and renders those strategies useless. It remains unknown how common crossflow is behind the pipe. It long has been suspected from other sources that crossflow between commingled reservoirs inside and outside the pipe is much more common in the Gulf of Mexico than elsewhere.

A limited number of production logs often confirms the presence of crossflow. This phenomenon can be expected to be more promi-

nent as wells age and severe stresses are placed on annular cement, especially in gas wells with increasing pressure differentials over time. Statistics from the Minerals Management Service (Sweatman, 2006) show that after a certain age, the majority of Gulf of Mexico wells is subjected to sustained casing pressure, and thus, poor well integrity is expected in as many as half of the existing wells. Finally, CO_2 sequestration poses additional challenges because CO_2 is notorious for washing out cement and corroding metal pipes (Powers, 2006). Leakage through various wellbore channels (Scherer, 2006) has been recognized as one of the biggest challenges in CO_2 sequestration. Yearly meetings of the Well Bore Integrity Network (http://www.co2captureandstorage.info/networks/wellbore-.htm) have been conducted since 2005 to address the problem, combining the forces of industry and academia.

Overall, we conclude that it might be likely that a large percentage of wells is affected by crossflow behind or inside the pipe. If this is the case, we should expect much more acoustic noise near and above active reservoirs. This also implies that placement of permanent seismic sensors in a production/injection well might be jeopardized. Because there are only a few permanent borehole seismic installations in the world, our knowledge about crossflow dynamics is very limited. However, further multidisciplinary studies are required to understand the extent of the described effects.

On the positive side, we could use permanent seismic/acoustic sensors to characterize crossflow in real time. Permanent seismic sensors can be thought of as a "stethoscope on the chest of the reservoir." They can detect early "coughing and sneezing," and appropriate "medicine" (workover) can be prescribed in a timely manner. In addition to crossflow, acoustic sensors can detect whistling of malfunctioning valves and sand particles coming in during sand production (Kringlebotn et al., 2006). Therefore, the "stethoscope" can differentiate between different "diseases" and be a multipurpose tool.

Another potential use of such sensors is illuminating the producing well with an active source that aims to monitor permeability along the completion. An example of such a technique, called real-time completion monitoring, given by Bakulin et al. (2008), relies on fiber-optic acoustic sensors placed across the sand face. Those same sensors can be used in a passive listening mode to diagnose crossflow, valve performance, sand production, and any other noises characteristic of producing wells. Therefore, we recommend pursuing a package of active and passive applications involving permanently installed acoustic sensors at the sand face.

CONCLUSIONS

For the first time, we report time-domain acoustic array measurements of flow behind the casing, which likely is caused by crossflow between two commingled reservoirs with different pressures and permeabilities. Reported conventionally as "noise" and measured only in the spectral domain, these acoustic signatures are a superposition of time-separated tube-wave arrivals with impulsive signatures, similar to those caused by air guns. Acoustic signatures excited by crossflow at the same depth are highly repeatable. Time-domain observation using the array allows use of powerful time-processing techniques. Recordings can be made above or below completed intervals, and arrivals from several sources of flow at different depths can be separated. Tube waves in microholes attenuate faster than in steel-cased wells. However, they can propagate for hundreds of meters, making possible the recording of noise large distances from noise-event locations. High frequencies of tube waves attenuate faster than low frequencies. This potentially can be used for discrimination between change of source location and source amplitude.

We have shown that acoustic signatures experience characteristic changes during repeated periods of air release and shut-in conditions. These changes seem to follow the repeated pattern and indicate repeated reversal in the direction of crossflow between two commingled reservoir units. Reservoir modeling confirms the possibility of such reversal from first principles. Results suggest that permanent real-time acoustic monitoring might allow better characterization of depletion in commingled stacked reservoirs.

ACKNOWLEDGMENTS

We thank Tom Daley, Ernie Majer, Ray Solbau, Alex Morales, and Roland Gritto (LBNL) for performing thorough work on geophysical acquisition. We are thankful to Steve Hardy, Dan Kelly, and Lori Kirby (Rocky Mountain Oilfield Testing Center, DOE) for field support and assistance. We thank Omer Alpak and Phil Fair (Shell) for their reservoir-modeling effort. We are grateful to Shell staff members Detlef Hohl, Jim O'Connell, Lorri Glassgold-Gibson, Bob Romero, and Mike Cowan for assistance. GeoKinetiK, LLC, provided imaging and processing software. We thank KinetiK Professional for real-time seismic data analysis.

APPENDIX A

RAW DATA AND AUDIO FILE OF ACOUSTIC SIGNATURES FROM CROSSFLOW

This electronic appendix contains two files. First is a text file (XflowREV.txt) containing a recording by a 20-level hydrophone array placed from 122-m to 217-m depth with 5-m spacing. First column is time in seconds, whereas remaining columns contain seismic traces. This record was done on April 21, 2005, after air injection at the end of the bleed-off period. The second file (Xflow_12.wav) con-

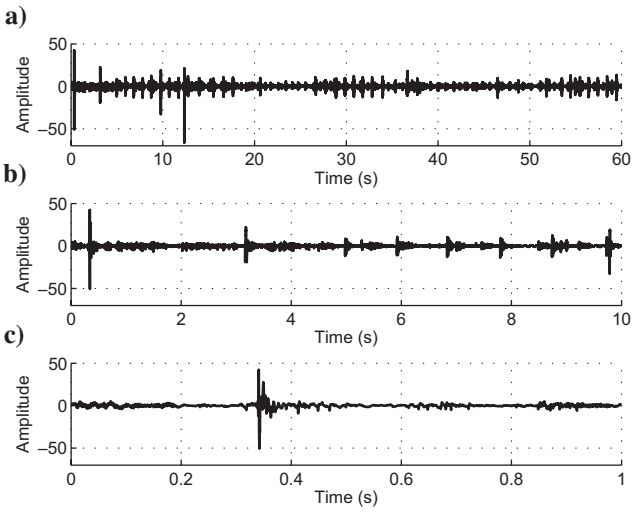

Figure A-1. Acoustic signatures of crossflow in the time domain. The audio file plays the entire 60-s seismic trace shown in (a). Display (a) shows the entire trace N 12 from data whereas (b) contains 10-s and (c) 1-s zoom-ins. [DOI: http://dx.doi.org/10.1190/1.2940154.1] [DOI: http://dx.doi.org/10.1190/1.2940154.2] Figure is enhanced online.

tains an audio record that corresponds to the trace N 12 depicted in Figure A-1. This audio is 60 s long and can be played on a computer.

REFERENCES

Bakulin, A., A. Sidorov, B. Kashtan, and M. Jaaskelainen, 2008, Real-time completion monitoring with acoustic waves: Geophysics, **73**, no. 1, E15–E33.

Chaudhry, A. U., 2003, Gas well testing handbook: Elsevier Science Publishing Company, Inc.

Kringlebotn, J. T., E. Rønnekleiv, and S. Knudsen, 2006, Apparatus for acoustic detection of particles in a flow using a fiber optic interferometer: U. S. Patent 7,072,044.

Knudsen, S., G. B. Havsgård, A. Berg, and T. Bostick, 2006, Flow-induced noise in fiber-optic 3C seismic sensors for permanent tubing-conveyed installations: 68th Annual Conference and Exhibition, EAGE, Extended Abstracts, D037.

McKinley, R. M., F. M. Bower, and R. C. Rumble, 1973, The structure and interpretation of noise behind the casing: Journal of Petroleum Technology, **3**, 329–338.

McCoy, J. N., 1962, Analyzing well performance: SPE Annual Technical Conference and Exhibition, paper SPE 337-MS.

Paillet, F. L., and J. White, 1982, Acoustic modes of propagation in the borehole and their relationship to rock properties: Geophysics, **47**, 1215–1228.

Powers, M., 2006, North Estes field in Texas: IEA Greenhouse Gas R&D Programme (IEA GHG), 2nd Well Bore Integrity Network Meeting, http://www.co2captureandstorage.info/networks/wellbore.htm, accessed May 10, 2006.

Raghavan, R., 1993, Well test analysis: Prentice-Hall, Inc.

Scherer, G., 2006, Corrosion of cement in simulated limestone and sandstone formations: IEA Greenhouse Gas R&D Programme (IEA GHG), 2nd Well Bore Integrity Network Meeting, http://www.co2captureandstorage.info/networks/wellbore.htm, accessed May 10, 2006.

Sweatman, R., 2006, API activity including sustained casing pressure and field and regional area studies: IEA Greenhouse Gas R&D Programme (IEA GHG), 2nd Well Bore Integrity Network Meeting, http://www.co2captureandstorage.info/networks/wellbore.htm, accessed May 10, 2006.

Tomutsa, L., S. R. Jackson, M. Szpakiewicz, and T. Palmer, 1986, Geostatistical characterization and comparison of outcrop and subsurface facies: Shannon shelf sand ridges: SPE Annual Technical Conference and Exhibition, paper SPE 15127.

U. S. Department of Energy, 2007, Microhole systems R&D, http://www.fossil.energy.gov/programs/oilgas/microhole/index.html, accessed July 3, 2007.

van der Spek, A., and A. Thomas, 1999, Neural-net identification of flow regime with band spectra of flow-generated sound: SPE Reservoir Evaluation and Engineering, **2**, no. 6, 489–498.